

The CDF MiniPlug Calorimeters ¹

Stefano Lami ²

(CDF Collaboration)

The Rockefeller University, New York, NY 10021-6399, USA

Abstract. Two MiniPlug calorimeters, designed to measure the energy and lateral position of particles in the (forward) pseudorapidity region of $3.6 < |\eta| < 5.2$ of the CDF detector, have been recently installed as part of the Run II CDF upgrade at the Tevatron $\bar{p}p$ collider. They consist of lead/liquid scintillator read out by wavelength shifting fibers arranged in a pixel-type towerless geometry suitable for ‘calorimetric tracking’. The design concept, the prototype performance and the final design of the MiniPlugs are here described. A recent cosmic ray test resulted in a light yield of approximately 100 pe/MIP, which exceeds our design requirements.

I INTRODUCTION

A program of hard diffraction and very forward physics proposed for CDF in Run II [1] requires the employment of two forward ‘MiniPlug’ calorimeters in the pseudorapidity region $3.6 < |\eta| < 5.2$ designed to measure the energy and lateral position of both electromagnetic and hadronic showers. The MiniPlugs extend the pseudorapidity region covered by the Plug Upgrade calorimeters ($1.1 < |\eta| < 3.5$) to the beam pipe. Using the MiniPlug and the Plug Upgrade calorimeters to actually measure the width of the rapidity gap(s) produced in diffractive processes will allow extending the Run I studies of the diffractive structure function to much lower values of the fraction ξ of the momentum of the proton carried by the Pomeron.

The MiniPlugs are based on lead/liquid-scintillator layers read out by wavelength shifting (WLS) fibers perpendicular to the lead plates and parallel to the proton/antiproton beams, arranged in a novel ‘towerless’ geometry (no boundaries between the fibers). The centroid of the fiber pulse height provides the position of the shower initiating particle. The desired number of fibers is then grouped and viewed by a single pixel of a multi-anode photomultiplier tube (MAPMT), providing what in the following we will call for simplicity a ‘tower’.

¹) Contributed paper to “DPF 2002, Section: New Detector Technologies”, Williamsburg, VA, May 24-28 2002

²) *E-mail address:* lami@physics.rockefeller.edu

As interacting hadrons release on average one third of their energy in the form of π^0 's, a short (few interaction lengths, λ) calorimeter can be used to measure the energy and position of both electrons/photons and hadrons. A set of fibers which do not sample the first 24 radiation lengths (X_0) of the detector can be used to tag hadrons.

The MiniPlugs have been installed downstream of the CDF Plug Upgrade calorimeters within the central hole of the muon toroids at a distance of 5.8 meters from the center of the detector (see fig. 1). Each MiniPlug is housed in a cylindrical steel vessel 26" (66 cm) in diameter and has a 5" (12.7 cm) hole concentric with the cylinder axis to accommodate the beam pipe. Due to the space constraints in the z -direction when the Plug is withdrawn to the "open" position to service the central detectors, the MiniPlug length is confined to 24" (61 cm). Within this length the actual calorimeters are $32 X_0$ and 1.3λ deep, and have no hadron tagging fibers.

The MiniPlug design combines a low cost construction with an efficient and high-resolution position determination. The design concept and MonteCarlo expectations are described in section II.

A $28 X_0$ prototype of cross section $15 \times 15 \text{ cm}^2$ was constructed in 1994 and tested first with 2, 3 and 5 GeV electron beams and an 8 GeV π^- beam at the Brookhaven National Laboratory (BNL) [2,3] and then with high energy positrons, muons and pions in the 1997 Fermilab test beam. The test results [4–6], summarized in section III, were found to be in good agreement with simulation predictions [7].

The final design of the MiniPlugs is described in section IV. Approximately, the design characteristics of passive and active materials were transferred from the prototype to the final design. In order to reduce the cost of the readout electronics, a coarser granularity was used, with a hexagonal cell structure about two times larger than the 4 cm^2 of the prototype. However, this was balanced by a higher number of fibers/cell (6 instead of 4) and a larger fiber diameter (1 mm instead of 0.83 mm). A cosmic ray test was performed, and its results are presented in section V, while first collider data are described in section VI.

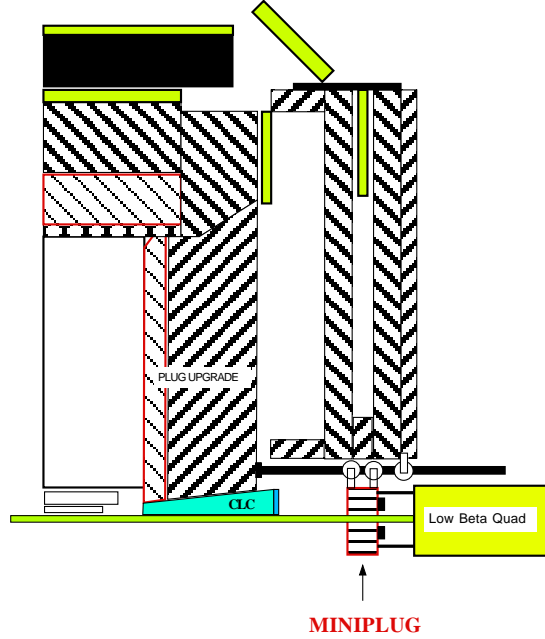


FIGURE 1. Schematic drawing of 1/4 view of the CDF detector showing a MiniPlug hanging from two unistrut beams supported on one end by the Plug and on the other by the toroid (not to scale). This scheme allows for moving the toroids and/or the Plug to access the central detector while the MiniPlug remains stationary.

II DESIGN CONCEPT AND GEANT SIMULATION

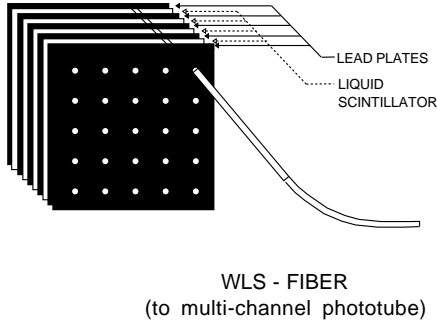


FIGURE 2. Conceptual design of the MiniPlug calorimeter: the fibers are arranged in a ‘towerless’ geometry, i.e. with no discrete tower boundaries.

but also for hadrons, which upon interaction release on average $1/3$ of their energy in the form of γ 's, mainly from $\pi^0 \rightarrow 2\gamma$ decays, which will interact again after $1 X_0$. So a several X_0 deep tracking calorimeter can be used, without a shower maximum detector, to measure the position and energy of both neutral and charged hadrons. For the MiniPlugs it is not convenient to be several λ long, to avoid the broadening of the hadron shower if a measurement of the particle position at the level of few millimeters is required.

We have studied the response of the MiniPlug calorimeters to single particles and jets in the CDF-II configuration by using a simulation based on the GEANT MonteCarlo program [8]. Each MiniPlug module comprised about $56 X_0$ and 2λ . The energy resolution for single particles was analyzed using beams of electrons and pions at incident particle energies between 10 and 100 GeV. The MiniPlug energy resolution for electrons is well described by the formula $\sigma/E = 18\%/\sqrt{E}$, where E is the incident particle energy in GeV. About 15% of the pions traversed the calorimeter module without interacting. For charged pions interacting in the Miniplug the energy resolution was found to be about 30%, independent of the pion energy; this is dominated by the fluctuation in the ratio π^0/π^\pm in the first interaction, independent of energy if the hadron shower is not contained.

The MiniPlugs consist of alternating layers of lead plates and liquid scintillator read out by WLS fibers. The fibers are inserted into an array of aligned holes drilled in the lead plates as shown in fig. 2 and are read out by MAPMTs. Effective ‘towers’ are formed by combining together the desired number of fibers to be viewed by a single pixel of a MAPMT.

For particles incident at small angles relative to the fiber direction, the fiber pulse height centroid provides the position of the shower initiating particle. Position determination is obtained not only for electrons and photons

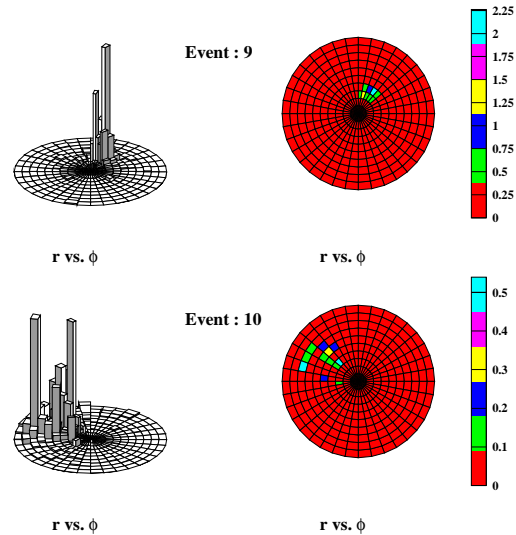


FIGURE 3. MiniPlug response to Monte Carlo generated jets. For each event an isometric lego plot (left) and color-coded front view (right) are shown.

Jets were generated using the HERWIG [9] MonteCarlo program. The jet energy resolution was studied by passing individual particles of a jet through the MiniPlug module and summing the response to each particle of the jet. Fig. 3 shows the MiniPlug response to typical jets. For each event an isometric lego plot (left) and color-coded front view (right) are shown. For convenience in representation, the impact point of a particle was expressed in polar coordinates r and ϕ relative to the center of the MiniPlug front surface. Figure 4 a) shows the distribution of the incident jet energy of the generated events. The distribution of the number of particles in a jet is presented in fig. 4 b). Figure 4 c) shows the percent fraction of the initial jet energy registered in the scintillator; from this distribution we evaluated the jet energy resolution to be $\sigma/E = 29.2\%$. The z -position of

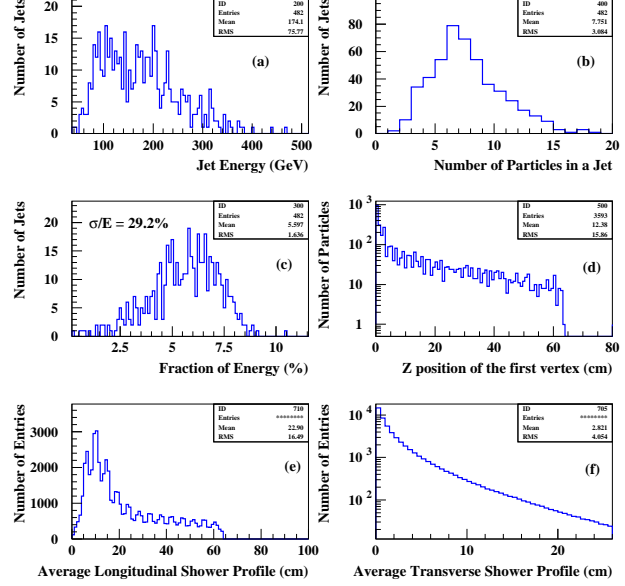


FIGURE 4. Distributions for jets incident on a 2λ MiniPlug obtained with a GEANT simulation.

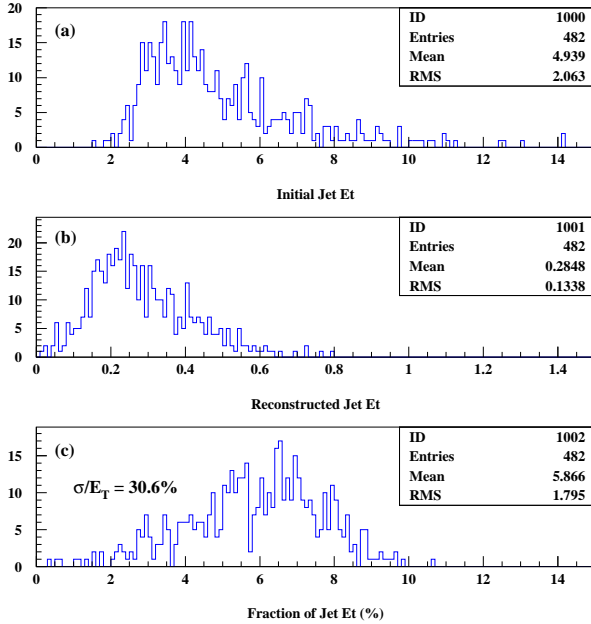


FIGURE 5. Jet E_T resolution in a 2λ MiniPlug obtained with a GEANT simulation: (a) Initial jet E_T distribution, (b) reconstructed jet E_T , (c) fraction of the initial jet E_T reconstructed in the MiniPlug.

the first shower vertex, the average longitudinal and transverse shower profile are shown in figures 4 d), 4 e), and 4 f), respectively.

Results for the jet E_T resolution in the MiniPlug are presented in fig. 5. The initial jet E_T distribution is shown in fig. 5 a), while the reconstructed jet E_T is plotted in fig. 5 b). Figure 5 c) shows the percent fraction of the initial jet E_T reconstructed in the MiniPlug, which yields a jet transverse energy resolution of 30.6% for the average E_T^{jet} of 4.9 GeV.

III THE PROTOTYPE PERFORMANCE

A schematic side view of the MiniPlug prototype is shown in fig. 6(left). The prototype consisted of 30 parallel lead plates, with dimensions $15\text{ cm} \times 15\text{ cm}$ and 4.8 mm thick, spaced 6.4 mm apart. The plates were laminated with 0.5 mm thick aluminum sheets of 86% reflectivity glued on the lead with epoxy. The same lead plate thickness and scintillator gap are used in the full scale MiniPlugs. Multiclad WLS Kuraray Y-11(350)M fibers of 0.83 mm diameter were inserted into an array of aligned holes in the plates through the entire depth of the detector. The holes have 1 mm diameter and were drilled with a CNC machine. The whole plate/fiber assembly was immersed in mineral oil based Bicorn 517L liquid scintillator. The MiniPlug prototype comprised about $28 X_0$ or about 1λ .

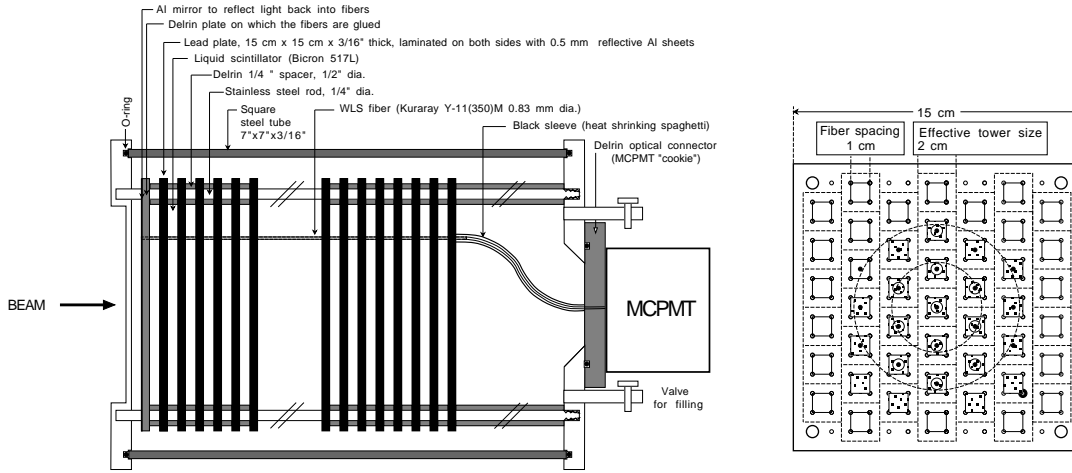


FIGURE 6. Schematic side view (left) and front view (right) of the MiniPlug prototype. Each group of four fibers in a square is read out by a single MAPMT channel. All the squares were instrumented at the 1997 test beam, as well as the single fibers at the center of the squares, as indicated (the shaded squares are those instrumented at the BNL test [3]).

In the prototype, the fibers were grouped as shown in fig. 6(right), with four fibers at the corners of a square read out by one MAPMT pixel, forming towers of effective size $2 \times 2\text{ cm}^2$. A reflective aluminum sheet was pressed against the far-ends of the fibers to reflect the light back into the fibers. The fibers in the centers of the squares were read individually. In an optimal design of a calorimeter of $\sim 2\lambda$ or $\sim 56X_0$, these single fibers would penetrate the calorimeter only through a certain distance from the back, stopping short of reaching the first $24 X_0$. In this way they would not be sensitive to electron/photon showers and therefore would provide a “*hadron tag*”. In the prototype these fibers were brought all the way to the front of the calorimeter to measure the expected light yield when tagging hadrons with one fiber per “tower”.

The MiniPlug operates by integrating the signal over several fibers within a distance determined by the effective attenuation length of the liquid scintillator, which depends on the number of reflections. Bench measurements yielded an effective at-

tenuation length of 20 mm for a scintillator thickness of 6 mm [3], which drove the choice of the tower size.

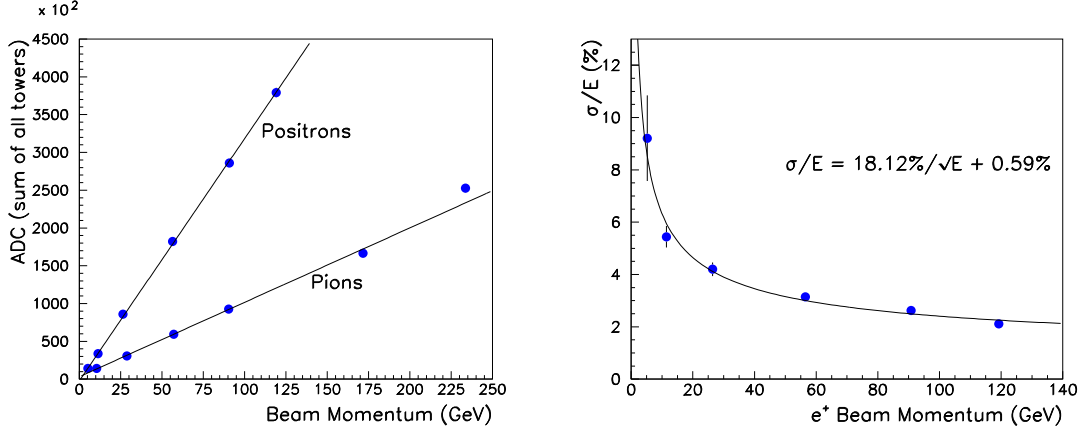


FIGURE 7. Left: The relation between ADC counts and beam momentum for positrons in the range 5-120 GeV and pions in the range 10-230 GeV, obtained in a beam test of the MiniPlug prototype, with the calorimeter plates perpendicular to the beams. Right: MiniPlug energy resolution for positrons.

The MiniPlug prototype was exposed to high energy positron, pion and muon beams at Fermilab in 1997. Sets of data were taken at angles of 0, 3 and 10 degrees between the beam and the calorimeter axis. The response of the prototype to positrons in the range 5–120 GeV and to charged pions in the range 10–230 GeV showed very good linearity. For positrons, the deviations from a linear fit were smaller than 1.5% (fig. 7, left) and the average energy resolution $\sigma/E = 18.1\% / \sqrt{E} + 0.6\%$ (fig. 7, right). For interacting charged pions the energy resolution was about 40%, independent of the pion energy. The lateral position resolution was measured to be $9.2 \text{ mm}/\sqrt{E}$ for positrons and $23.8 \text{ mm}/\sqrt{E}$ for pions (fig. 8).

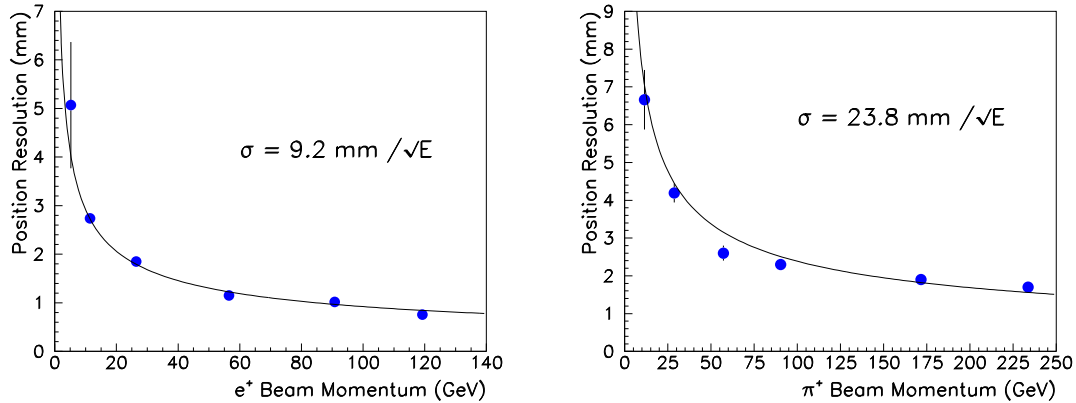


FIGURE 8. MiniPlug prototype position resolution for positrons in the range 5-120 GeV (left) and pions in the range 10-230 GeV (right).

IV MINIPLUG FINAL DESIGN

A schematic drawing of a side view of a MiniPlug is presented in fig. 9. The active calorimeter consists of 36 lead-based plates separated by 1/4" spacers and immersed in liquid scintillator. Table 1 summarizes various parameters of the MiniPlug calorimeters.

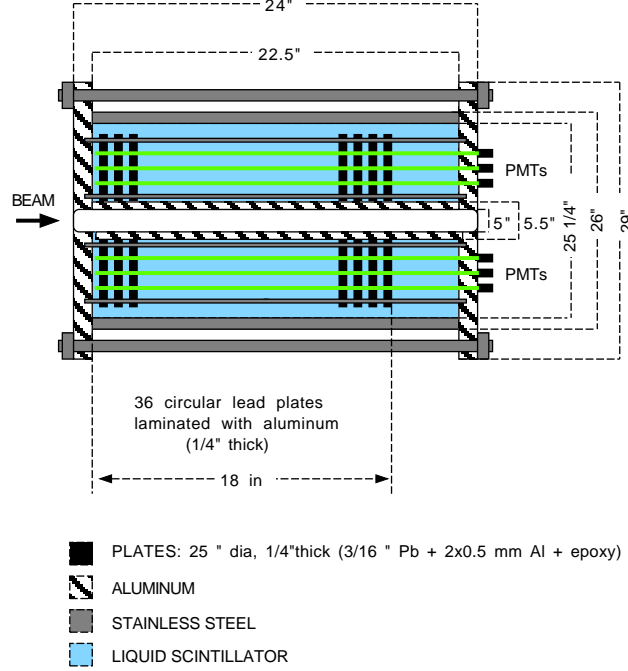


FIGURE 9. Schematic side view of a Miniplug (not to scale).

The calorimeter plates were manufactured by Alchemy Castings Inc. [10]. They are 25" (63.5 cm) in diameter and are made of 3/16" thick (Pb+6% Sb) alloy laminated with 0.5 mm Al of 80% reflectivity. Each plate has 1512 holes for the

TABLE 1. Parameters of the MiniPlug calorimeter.

Sensitive length	571.5 mm
Inner sensitive radius	139.7 mm
Outer sensitive radius	641.4 mm
Weight	840 Kg
Depth (including Al flanges)	609.6 mm
Thickness	$32 X_0, 1.3 \lambda$
Number of plates	36
Plate thickness	4.8mm (Pb+6% Sb) + 1mm Al
Scintillator gap thickness	6.4 mm
Scintillator	Bicron 517L
Wavelength shifter	Kuraray Y11 1mm dia.
Phototube	Hamamatsu R-5900 M16
Number of WLS fibers/pixel	6
Number of phototubes	18

fibers, drilled with a #54 (or 1.4 mm) drill and chamfered. In addition, 12 holes of 1/4" and 6 holes of 1/2" nominal diameter are used for ‘hanging’ the plate in its final position in the calorimeter from stainless steel rods supported by the MiniPlug end plates, as seen in fig. 9. A MiniPlug plate is $0.86 X_0$ and 0.03λ thick, and weighs 21 Kg. The active length of a MiniPlug, including the liquid scintillator, is $32 X_0$ and 1.3λ , and the total weight, including the liquid scintillator, is approximately 840 Kg (1850 lbs). Because of the mentioned space limitations, the final design has no hadron tagging fibers.

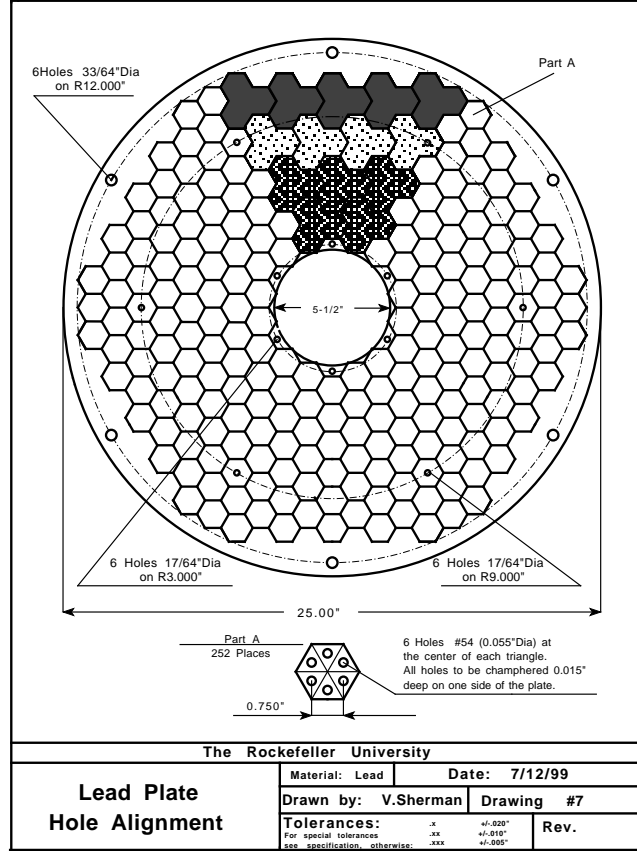


FIGURE 10. MiniPlug lead plate. The tower design is based on a hexagon geometry. Each hexagon has six holes, with a WLS fiber inserted in each hole. The six fibers of a hexagon are grouped together and are viewed by one MAPMT channel. There are 252 hexagons in each MiniPlug viewed by 18 16-channel MAPMTs. The MAPMT outputs are added in groups of 3 to form 84 calorimeter ‘towers’.

Figure 10 shows the layout of the fiber holes in a Miniplug plate. The design is based on a hexagon geometry. Each hexagon has six holes, as shown. A WLS fiber is inserted in each hole. The six fibers of a hexagon are grouped together and are viewed by one MAPMT channel. A seventh fiber, which is clear and carries the light from a calibration LED, is also read out by each MAPMT pixel. There are 252 hexagons in each MiniPlug viewed by 18 16-channel MAPMTs. The MAPMT outputs are added in groups of 3 to form 84 calorimeter ‘towers’. The

single hexagonal cells could eventually be read out individually. Presently we read out 84 towers per MiniPlug and the summed MAPMT outputs (18 channels per MiniPlug), amounting to a total of 204 channels for the two MiniPlugs. The towers viewed by the three MAPMTs of a sextant are shown in fig. 10 with different shades.

We use Bicorn 517L liquid scintillator [11] and Kuraray Y11 (350) multiclad 1.0 mm dia. WLS fibers read out by Hamamatsu R5900-M16 MAPMTs [12].

The Bicorn 517L liquid scintillator, also used in the prototype, is a mineral oil with Pseudocumene as the active ingredient. Because of its high chemical compatibility with polystyrene based fibers, low cost and radiation hardness, the BC-517L scintillator had been considered and studied extensively for applications at the Superconducting Super Collider (SSC).

In the MiniPlug prototype we used one 0.83 mm dia. fiber per cm^2 , and grouped four fibers together to form a ‘tower’ of effective area 4 cm^2 . In the final MiniPlug design, there is one fiber per 1.6 cm^2 , but the 1 mm dia. of the fibers compensates for the reduction in light expected due to the larger area covered by each fiber. Moreover, the fibers are now aluminized at the ‘far end’, while in the prototype they were pressed against a reflective plate.

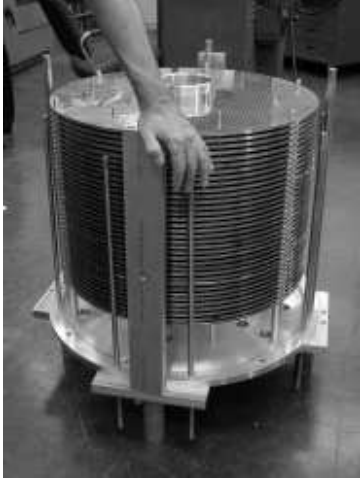


FIGURE 11. A dry stack of the plates of a MiniPlug.

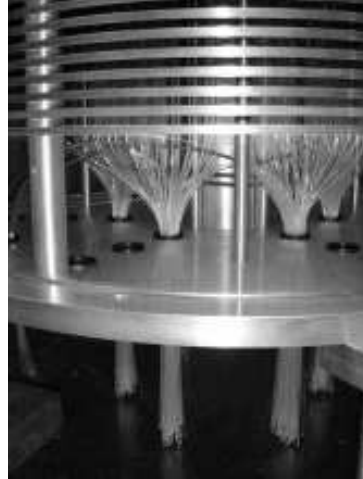


FIGURE 12. A view of the fiber routing.

The Hamamatsu R5900-M16, a 16 channel tube, was selected because of its relatively low cost per channel and acceptable channel to channel gain uniformity.

The expected radiation dose in the MiniPlugs in Run II has been estimated to be $\sim 30 \text{ KGy}$ (3 Mrad) per year. Such a dose is not expected to affect the response of the liquid scintillator. SSC studies on WLS fibers showed that the permanent damage in light transmittance of 1.0 mm dia., 1 m long fibers is about 10% after an irradiation of 64 KGy [13]. Radiation hardness studies performed for the Large Hadron Collider (LHC) showed that Kuraray Y11 fibers were the least damaged when compared to other commercially available fibers [14]. The standard

borosilicate glass of MAPMT windows is sensitive to radiation and, when tested in connection with SSC applications, showed a 60% relative transmittance at 500 nm for a 30 K Gy dose. For this reason, the R5900 MAPMTs for the MiniPlugs were ordered with a quartz window, which substantially improves the MAPMT radiation hardness.

The two MiniPlug calorimeters have been assembled at Rockefeller. Fig. 11 shows a dry stack of the plates of a MiniPlug, and a view of the fiber routing is shown in fig. 12. After the fibers have been sealed into the optical connectors on the back plate, they have been cut with a diamond string-saw, and the connector surface hand polished. Fig. 13 shows one MiniPlug at Fermilab before installation. On the back plate are mounted 18 MAPMTs, plus two LED assemblies for calibration.



FIGURE 13. A MiniPlug at Fermilab before installation.

V COSMIC RAY TEST

We tested a 60° section of one MiniPlug using cosmic ray muons. In the first step we determined the channel response uniformity (and the operating voltage) of the tubes to be used on the MiniPlugs. Then the single photoelectron response was measured using a ^{60}Co gamma source. Finally, a cosmic ray trigger was made of a 2-fold coincidence of two scintillation counters mounted above and below the MiniPlug module. The front-end readout system employed for these tests was a CAMAC based LeCroy 2249W [15] 11-bit 12-channel charge integrating ADC, with a sensitivity of 0.25 pC/count, controlled by a National Instrument ‘Labview’ [16] data acquisition software.

A Photomultiplier Test

The light carried by the WLS fibers is read out by 16-channel Hamamatsu H6568-10/R5900 M16 tubes [12], whose cross section has a size of about one square inch and whose specifications are listed in Table 2. In addition to the 16 anode channels, these MAPMTs have a channel which is the sum of the last dynodes of all 16 channels. The output of this channel will be referred to as the ‘sum-output’.

TABLE 2. Characteristics of the Hamamatsu H6568/R5900 M16 photomultiplier tubes specified for the MiniPlug calorimeter.

Parameter	Description/Value
Window material	quartz
Quantum efficiency at 500 nm	$\geq 13\%$
Anode dark current	1 nA
Pulse linearity per channel ($\pm 2\%$ deviation)	0.5 mA
Cross-talk	1 %
Uniformity between each anode	1:2.5
Photocathode material	bialkali
Spectral response	300 ~ 650 nm
Number of stages	12
Anode	array of 4×4
Pixel size	4 mm \times 4 mm
Maximum high voltage	1000 V
Anode pulse rise time	≤ 1 nsec

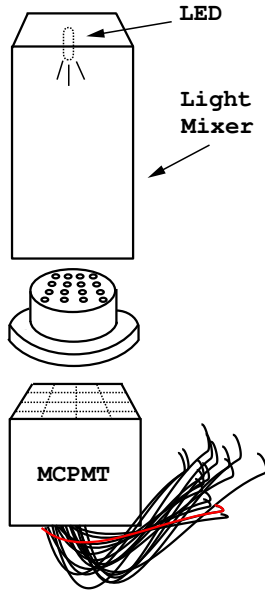


FIGURE 14. The setup of the MAPMT test system uses a green LED embedded in a light mixer to distribute the light uniformly into the 16 channels of the MAPMT.

The setup we used for measuring the relative response of the MAPMT channels is shown in fig. 14. A green LED is placed in a hole drilled at one end of a rectangular lucite bar, which acts as a ‘light mixer’ distributing the LED light uniformly among a set of clear fibers mounted in holes drilled in a delrin ‘cookie’ in a pattern matching that of the MAPMT photocathode pixels. There are 7 fibers in each cookie hole, just as in the final MiniPlug design. The uniformity of the LED light across the 4×4 cookie channels has been measured with three MAPMTs, and the measurement has been repeated after rotating each tube by 90° , 180° and 270° . Since at each rotation a given MAPMT pixel is illuminated by a different cookie channel, the differences among ADC counts

obtained at the four settings reflect the differences in illumination of the corresponding cookie channels. These measurements show a standard deviation of $\pm 3\%$. Finally, the operating voltage of the tubes has been determined by equalizing the sum-outputs. The desired gain for the tubes operating in the MiniPlugs is 10^5 which, according to the manufacture’s specifications, is achieved at a MAPMT voltage of approximately -700V. The LED light was adjusted to bring the sum-output of one PMT, whose voltage was set to yield a gain of 10^5 , to 450 ADC counts. Then, for each one of the other tubes, the high voltage was varied in steps

of ± 10 V in the range from -600 to -800V to find the value at which its sum-output was closest to 450 ADC counts. Variations around the average value -700V were about ± 5 %.

The response of the 16 channels of each MAPMT to the illumination of the LED in the setup of fig. 14 was measured and compared with the specifications supplied by the manufacturer. In the MiniPlugs, the MAPMT channels has been hard-wired into groups of 3, forming 5 ‘grouped channel’ triplets and one singlet per MAPMT (the latter, channel #16, will not be read out in the MiniPlugs). Therefore, a special connector was made to group the MAPMT channels in the test setup, and the response of the 5 grouped channels was also measured. The test results for one MAPMT are shown in fig. 15: (a) relative response of the 16 channels, defined as the ratio of the pulse height of a channel to the maximum pulse height of all 16 channels; (b) measured relative channel response compared to values obtained from the manufacturer; (c) relative response of grouped channels; and (d) the difference between the relative response of a grouped channel and the expectation from the measurement of the 16 individual channels.

The ‘uniformity’ index of the 45 tested MAPMTs, defined as the ratio of the lowest to the highest channel response, showed an average value of 2.1 ± 0.3 .

Since the sum-output will be used as a trigger, it is also important to study the correlation between the sum of outputs from the 16 individual channels and the sum-output. We found that the ratio of the sum of outputs from the 16 individual channels to the sum-output is constant in the range of about $10 \sim 1000$ pC.

B Single Photoelectron Measurement

A measurement of the signal from single photoelectrons was carried out using a ^{60}Co gamma source, which was placed just outside the MiniPlug vessel. The light emitted by the liquid scintillator when irradiated by the source is rather weak and usually results in single photoelectron emission by the MAPMT photocathode. We

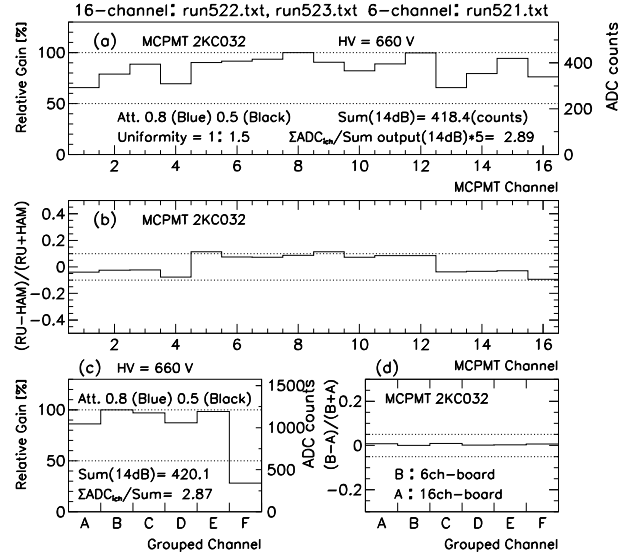


FIGURE 15. (a) Relative response of the 16 channels of one MAPMT; (b) difference between measured relative response and values provided by the manufacturer; (c) relative response of grouped channels; (d) difference between relative response of grouped channels and the expectation from the measured response of the individual channels.

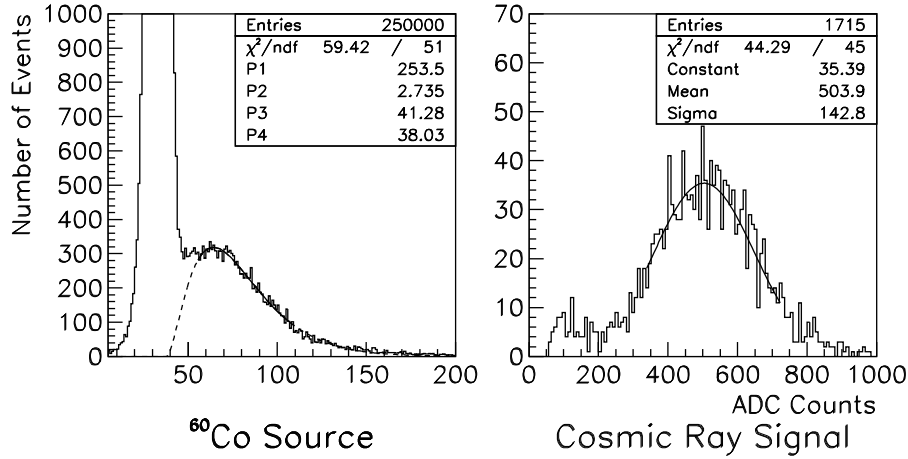


FIGURE 16. Left: the ^{60}Co source signal for a single tower. The data are fitted with a *Polya distribution*, $P(m) = [m(mG/G_0)^{m-1} \cdot e^{-mG/G_0}]/\Gamma(m)$. The parameter $p3 = G_0$ corresponds to the pulse height for single photoelectrons. Right: the cosmic ray spectrum with the isolation cut fitted with a Gaussian function.

triggered events using a randomly-generated gate of width $1 \mu\text{s}$. Most triggers do not contain any signal within the gate, but a small fraction of events have a single photoelectron signal.

Three MAPMTs to read out one 60° section of one MiniPlug were operated at -960V in this cosmic ray test, corresponding to a gain of $\sim 5.0 \times 10^6$ as specified by the manufacturer. At this gain, the expected single photoelectron response of the LeCroy 2249W ADC unit is approximately 3.2 counts. A LRS 234 linear amplifier [17] was used to amplify the signal by a factor of 10.

Figure 16(left) shows the ^{60}Co source signal for one tower, with a clear single photoelectron peak. The distribution has been fitted with a *Polya distribution*, i.e.

$$P(m) = \frac{m(mG/G_0)^{m-1}}{\Gamma(m)} \cdot e^{-mG/G_0}$$

which is the appropriate one for describing single photoelectron pulse height distributions. In the fit, $p1$ is the normalization constant, $p2$ the parameter m , $p3$ the parameter G_0 , and $p4$ the pedestal mean value. We obtain $41.28/10=4.1$ ADC counts for the single photoelectron response of this tower. Similar results were obtained from the other tested towers.

C Cosmic Ray Test Results

The cosmic ray trigger was made of a 2-fold coincidence of two scintillation counters mounted above and below the MiniPlug module. The scintillation counters were read out by RCA 8575 PMTs.

A better separation of the cosmic ray muon peak from the pedestal is obtained by plotting the tower response after imposing an isolation cut which requires that

the adjacent towers have a signal smaller than their own cosmic ray muon signal. Figure 16(right) shows the signal distribution after the isolation cut. Even with the isolation cut, the cosmic ray muon path length differences within a given tower still contribute to the width of the muon peak. So, although a cosmic ray muon spectrum is expected to follow a Landau distribution, the measured distribution is a sum of several different Landau distributions and is better described by a Gaussian function to obtain the ADC counts for the cosmic ray muon peak, as shown in fig. 16(right). The mean value of the cosmic ray signal distribution for the tested towers has been measured to be about 400 photoelectrons. Dividing these values by the corresponding single photoelectron ADC counts we obtain on average more than 100 photoelectrons/MIP for a single tower.

VI FIRST COLLIDER DATA

The MiniPlugs were installed in the the CDF apparatus few months ago, and were operated stably and reliably since then. However, they are not fully instrumented yet. At the time of writing, only the sum-output (the 17th channel) of each tube is read out. This means a coarser granularity for the present, equivalent to 18 towers per MiniPlug. Figure 17(left) shows, as a $\phi - \eta$ lego-plot, the average ADC counts from a Collider run. The inner ring of towers, at higher pseudorapidity, has larger signals. That is in agreement with results obtained with the MBR Minimum-Bias event generator [18], followed by a parameterization of the detector response, as shown in fig. 17(right).

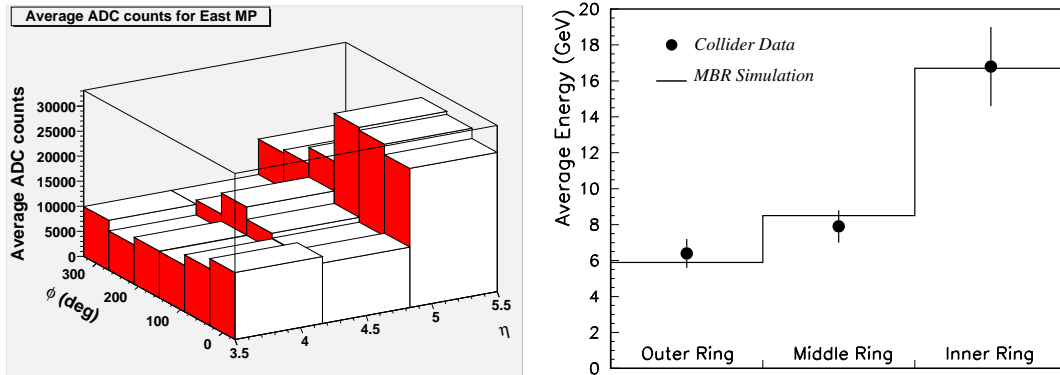


FIGURE 17. Left: the average ADC counts from a Collider run, for the 18 towers of a MiniPlug currently read out. Right: Collider data are compared to an MBR simulation for the three different pseudorapidity rings.

VII CONCLUSIONS

Two MiniPlug calorimeters, designed to measure the energy and lateral position of particles in the forward region ($3.6 < |\eta| < 5.2$) of the CDF detector, have been recently installed as part of the Run II CDF upgrade at the Tevatron $\bar{p}p$ collider.

They consist of lead/liquid scintillator layers read out by WLS fibers arranged in a pixel-type towerless geometry. In this paper we described the final design of the MiniPlugs and presented results from a cosmic ray test, in which a light yield of approximately 100 pe/MIP was obtained, exceeding our design requirements. First Collider data show a detector response in agreement with expectations.

REFERENCES

1. Fermilab Proposal 916 (1999).
2. Q.F. Wang, “*Pixel Array Detector for Forward Calorimetry*”, Proc. of the Vth Int. Conf. on Calorimetry in High Energy Physics, Brookhaven National Laboratory, 25 September-1 October 1994, 394.
3. S. Bagdasarov, K. Goulios, A. Maghakian, Q.F. Wang, “*Test-beam Results of a Prototype Position Sensitive Towerless Calorimeter*”, *Nucl. Instrum. Methods* **A372** (1996), 117.
4. K. Goulios and S. Lami, “*Performance of a Prototype Position Sensitive Towerless Calorimeter at the 1997 CDF Test Beam*”, Proc. of the VIIth Int. Conf. on Calorimetry in High Energy Physics, Tucson, Arizona, 9-14 November 1997, 307.
5. K. Goulios and S. Lami, “*Proposed Forward Detectors for Diffractive Physics in CDF-II*”, Proc. of the “Diffractive Physics, LAFEX International School on High Energy Physics (LISHEP-98)”, Rio de Janeiro, Brazil, 10-20 February 1998; FERMILAB-CONF-98/111-E.
6. K. Goulios and S. Lami, “*Performance of a Prototype Position Sensitive Towerless Calorimeter*”, *Nucl. Instrum. Methods* **A430** (1999), 34.
7. S. Bagdasarov and K. Goulios, “*Calorimetric Tracking of High Energy Particles*”, Proc. of the IVth Int. Conf. on Calorimetry in High Energy Physics, La Biodola, Isola d’Elba, Italy, 19-25 September 1993, 524.
8. R. Brun et al., GEANT Detector Description and Simulation Tool, CERN Program Library, W5013, 1994.
9. G. Marchesini et al., *Comp. Phys. Comm.* (1992) 465.
10. Alchemy Castings Inc., 563 Kenilworth Ave N, Hamilton, Ontario L8H 4T8;
<http://www.alchemycastings.com>
11. <http://www.bicron.com/bc517L.htm>
12. <http://usa.hamamatsu.com/cmp-detectors/arrays/pmt/Default.htm>
13. K.G. Young et al., “*Radiation and Solvent Effects on WLS Fibers used with Liquid Scintillators*”, Proc. of the Int. Conf. on Radiation-Tolerant Plastic Scintillators and Detectors, Radiation Physics and Chemistry **41** (1993), 215.
14. The ATLAS/Tile Calorimeter Collaboration, “*ATLAS Tile Calorimeter, Technical Design Report*”, CERN/LHCC 96-42 (1996).
15. <http://www.lecroy.com/lrs/dsheets/2249.htm>
16. <http://www.ni.com/labview/>
17. <http://www-esd.fnal.gov/esd/catalog/main/lcrynim/234-spec.htm>
18. F. Abe et al., *Phys. Rev. D* **50**, 5535 (1994); *D* **50**, 5550 (1994).